Chalcogenide Letters Vol. 21, No. 6, June 2024, p. 459 - 473

Optical and radiation shielding characteristics of Dy_2O_3 doped B_2O_3–TeO_2–BaO glasses

S. H. Farhan*, B. M. Al Dabbagh, H. Aboud
Applied Sci. Department, University of Technology, Iraq, college of sci., Al-Mustansiriya University, Iraq.

Glass samples with varying compositions was prepared by standard approach. The composition of the samples was (50-x) B_2O_3–$25TeO_2$–25BaO-xDy_2O_3, with x ranging from 0 to 1.25 mol%. XRD profiles confirmed that the samples were amorphous, as there were no long-range lattice arrangements observed. The successful preparation of amorphous samples was further confirmed by the absence of sharp lines & peaks. The optical properties of the obtained samples were analyzed. That a decrease in E_{opt} values resulted in a higher value of the refractive index (n) for the glasses. However, when the concentration of Dy_2O_3 exceeded certain levels (0.75, 1, and 1.25 mol%), the refractive index (n) decreased due to an increase in E_{opt} values. Experimental measurements using a NaI(Tl) detector were conducted to determine the radiation shielding parameters (LAC and MAC), as well as the (HVL), (TVL), & (MFP) of the glasses against gamma rays emitted by ^{137}Cs and ^{60}Co isotopes at energies of 0.662, 1.173, and 1.333 MeV. Excellent agreement was observed when comparing the experimental results with theoretical calculations using Phy-x/PSD software program. This suggests that the fabricated glasses have great potential for various applications in the field of optics and can effectively shield against radiation.

Received March 2, 2024; Accepted June 12, 2024)

Keywords: Optical and radiation shielding properties, Absorption spectrum fitting (ASF), Radiation parameters, Optical band gap, Refractive index

1. Introduction

Over the years, improvements in the technologies have undoubtedly contributed to humans' ability to complete numerous tasks while saving time, effort, and cost. However, this advancement has led to numerous health hazards to human. In fact, uses of radiation are now widespread for various purposed like environmental conservation, growth facilitation, food production, research, and healthcare [1]. In various applications, such as medical imaging or industrial processes by gamma rays and X-rays, it is crucial to select suitable safety materials to shield against harmful radiation and ensure the security of radiation sources. [2]. Despite their many disadvantages, various low-cost common practice to use concrete for the purpose of shielding against radiation. because of their ability to be shaped into different geometries [3]. Prolonged exposure to nuclear radiation causes cracks, reduced density[4]. In addition to that, the strength of concrete materials can be influenced by the amount of water trapped within them as well as any chemical destruction posing a significant challenge as workers are unable to reach the interior of such structures. Glasses are being studied by researchers as a possible material for radiation shielding because of their ability to absorb γ-rays and neutrons, as well as their high visibility [5]. Glass materials have been proven to be effective radiation shields by several authors. The ability of a material to protect against radiation depends on several factors, including (LAC and MAC), atomic number and electron density, (MFP), and more. It is crucial to accurately evaluate these parameters. [6, 7]. A comprehensive survey of recent literatures revealed that the shielding and radioactivity properties of glass have been the subject of intense investigations. A study conducted by El-Mallawany et al; [8] focused on the ability of tellurite glass as a shielding

* Corresponding author: as.21.25@grad.uotechnology.edu.iq
https://doi.org/10.15251/CL.2024.216.459

material.to evaluate the safety features of the glasses by analysing their optical and gamma protection properties. Due to their specific properties, these glasses have a variety of uses, especially in optics and photonics. Several researchers have become more interested in TeO_2 based glasses due to their appealing characteristics, which include low melting points, The features include strong radiation protection, great thermal stability, superb infrared transmission, high relative permittivity and low photon energy. [8, 9]. TeO_2-based glasses materials possess high refractive indices, making them highly desirable for various applications in the field of optics. These glasses are particularly suitable for the production of solar cells, as their high refractive indices enable efficient light trapping and absorption. Moreover, the high refractive indices of TeO_2-based glasses facilitate the development of solid-state lasers, as they enhance the efficiency of light amplification and enable the generation of high-power laser beams. Additionally, their nonlinear properties make them ideal for optical fibre applications, enabling the transmission of signals over long distances with minimal losses. Overall, the unique optical properties of TeO_2-based glasses make them versatile and valuable materials for advanced technologies in energy and telecommunications systems.[8, 10]. In addition, TeO_2 exhibits an exceptional capacity to bond with virtually any kind of glass, resulting in the creation of innovative compositions in tellurite glass systems[11]. Conversely, when rare earth ions are added to tellurite glasses, they exhibit broad emission bands materials and extended lifetimes under excitation. These materials are ideal for enhancing luminescent properties as host materials.[12]. In glasses, the inclusion of rare-earth elements like erbium (Er), neodymium (Nd), ytterbium (Yb), and dysprosium (Dy) as dopants is a common practice to introduce specific optical characteristics like near-infrared laser emission and amplification. with high atomic numbers and densities are often selected for gamma-ray shielding [13]. Ramman and other's[14] prepared bismuth Boro tellurite glasses doped with ytterbium oxide and determined its nuclear shielding properties and optical energy band gaps. The evaluation process involved gamma radiation shielding properties were investigated. Considering the radiation protection potential of tellurite glass system, in this study the safety properties of (50-x) B_2O_3–25TeO_2–25BaO-xDy_2O_3 (x = 0, 0.25, 0.5, 0.75, 1, and 1.25 mol%) glasses were evaluated. The glasses that were obtained underwent characterization to assess their structural properties, optical traits, and ability to shield gamma radiation and to further validate the results of shielding, a comparison was made between the experimental data and the values calculated theoretically.

2. Experimental procedures

Chemically pure raw materials (as glass constituents) in powder form were used to synthesize all the glass samples using conventional method, employing various compositions (50-x) B_2O_3–25TeO_2–25BaO-xDy_2O_3 (x = 0, 0.25, 0.5, 0.75, 1 and 1.25 mol%) and its coded as BBTD0%, BBTD0.25%, BBTD0.5%, BBTD0.75% BBTD1%, BBTD1.25% .Various raw materials to each glass sample were prepared by accurately weighing the initial mix all the previously weighed chemical material is carefully placed into a platinum crucible then was placed in furnace at approximately 965-970°C for half hour then were shaken often to get rid of bubbles and make a smooth melt. In order to prevent cracking, the glass sample underwent annealing at 300 °C for three hours approximately following the rapid cooling of the melt then proud onto a mould made of stainless steel. Using silicon carbide paper, the surface of the glass samples was polished to obtain a smooth, clear and parallel surface (Figure 1).

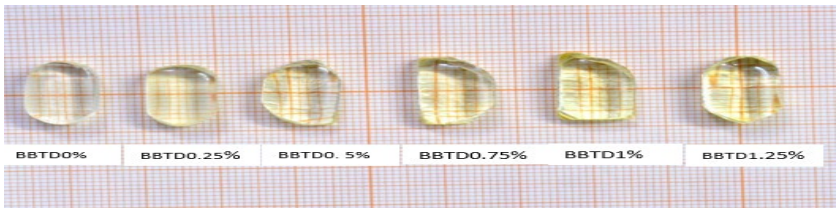

Fig. 1. Image of the fabricated glass system.

3. Results and discussion

3.1. XRD

Figure 2 exhibit the XRD profiles of the samples. The lacking regular patterns of atoms arranged over long distances. in the sample with a broad hump indicated their amorphous nature. Absence sharp lines and peaks confirmed the successful preparation of amorphous samples wherein sharp Bragg diffraction peaks cannot be observed in glasses due to the non-uniform spacing between atoms [15, 16].

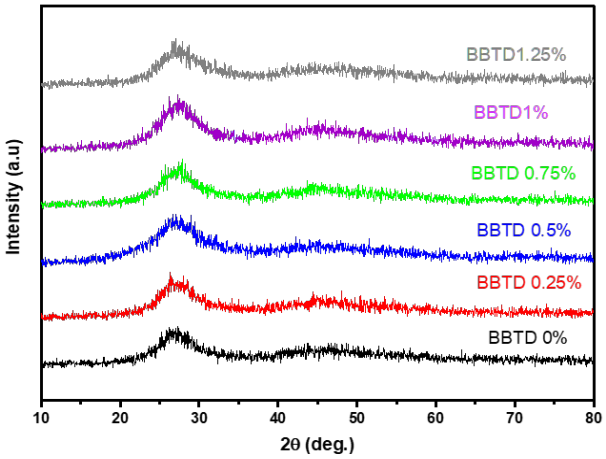

Fig. 2. XRD profiles of all prepared B_2O_3–TeO_2–BaO-Dy_2O_3 samples.

3.2. Optical properties of prepared glasses via Tauc's and ASF model

Figure 3 displayed the absorption spectra of the glasses wherein the UV-Vis absorption edge was moved towards lower wavelengths as the Dy_2O_3 content were increased. Figure 4 shows the Tauc's plot [17] [18] for an indirect transition across the band gap. The absorption coefficient α(ν) was calculated using following equation [19] given by:

$$\alpha(\upsilon) = \frac{A(h\nu - E_{opt})^p}{h\nu} \quad (1)$$

The ASF model [17, 20] an assessment was conducted E_{gap}^{Indir} of the specimen, without thickness information of the samples is not provided, the ASF model can still estimate their E_{opt} based on the absorption spectral data. Figure 3 was used to determine the cut-off wavelength (λ_{cut}) for each spectrum, thus obtaining the E_{opt} of the glasses. The linear part of the Tauc plot was extrapolated at zero absorbance to get the values of λ_{cut} . $E_{Band}^{Tuacs,indirct}$ of each glass was calculated via [21]:

$$E_{gap}^{Indir} = \frac{hc}{\lambda_{cut}} = \frac{1239.83}{\lambda_{cut}} \quad (2)$$

Through the $E_{Band}^{Tuacs,indirct}$ examination of the curves depicting energy (E) values on the x-axis and $(\alpha h\nu)^{1/2}$ values on the y-axis, we are able to determine the band gap of each sample. The obtained values of $E_{Band}^{Tuac\,s,indirct}$ and $E_{Band}^{ASF,indirct}$ for the glasses made with Dy_2O_3 contents of 0, 0.25, and 0.5 glasses were reduced, whereas for glasses made with Dy_2O_3 contents of 0.75, 1, and 1.25 were increased. The values of E_{opt} for two methods (Tauc's and ASF) are clearly presented in Table 1 and showed in figure 4 and 5 respectively. There is a clear correlation between $E_{Band}^{Tuac\,s,indirct}$ and $E_{Band}^{ASF,indirct}$ values of BBTD glass, as depicted in Figure 6 .More trigonal units (TeO_3) were transformed into tetrahedral units (TeO_4) with increasing Dy_2O_3 contents in the glass

network, increasing the E_{gap}^{Indir} [22]. The observed shift in the optical absorption edge towards higher energies indicated an increase in the glass matrix cross-linking density, improving the oxygen bond strength within the glass matrix [23]. In the meantime, as more BO_3 units were converted to BO_4 units, there was a decrease in the number of (NBO) atoms while bridging oxygen (BOs) atoms increased. Consequently, the greater amount of Dy_2O_3 contents caused a rise in the number of closely interconnected anions within the host network, resulting in an increased value of $E_{opt.}$ [24]. Previous studies have also reported the same behaviour [25, 26].

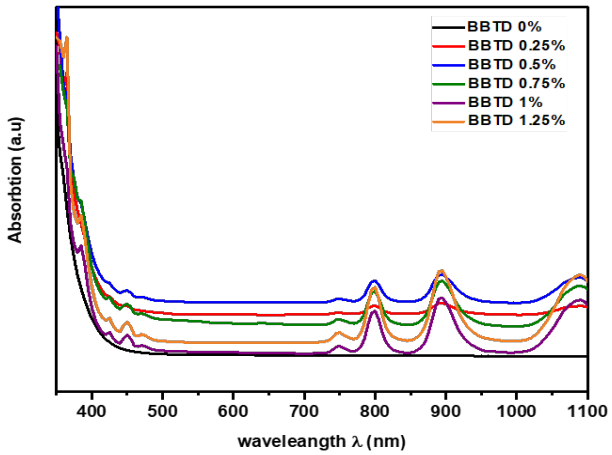

Fig. 3. Optical absorption spectrum of the proposed glasses.

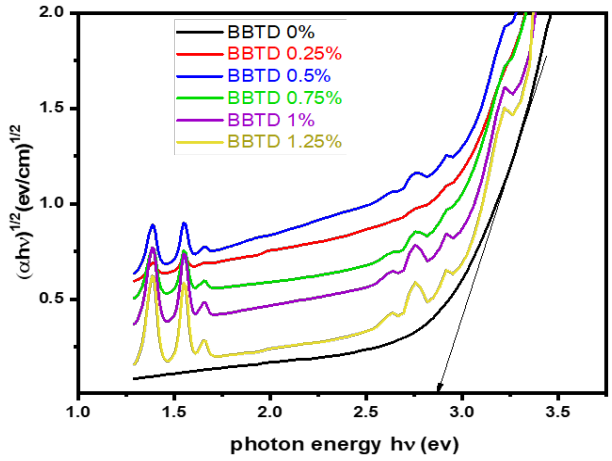

Fig. 4. Band gap of glasses using Tauc's plot.

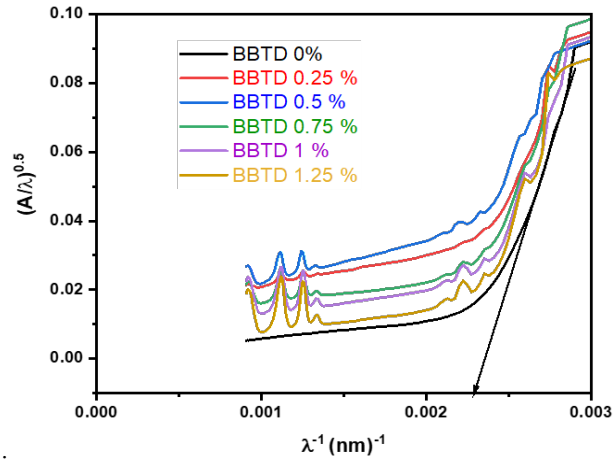

Fig. 5. Band gap of glasses using ASF plot.

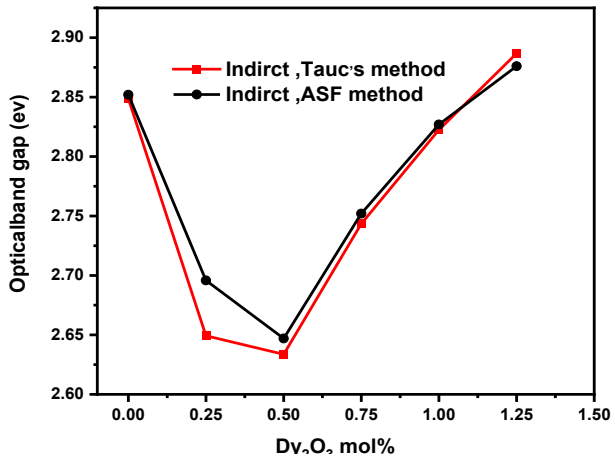

Fig. 6. Correlation between $E_{Band}^{Tuac\ s,indirct}$ and $E_{Band}^{ASF,indirct}$ values of BBTD glass vs Dy_2O_3 mol%.

The refractive index (n) of glasses is significant that determines its performance in different applications. Tauc and ASF methods was used to evaluate the values of n for the studied glasses [27] wherein indirect allowed optical transitions were considered. The decrease in the values of E_{opt} caused an increase in the values of n of the glasses. However, at high content of Dy_2O_3 (0.75, 1 and 1.25 mol%), the value of n was decreased as the values of E_{opt} were increased. Table 1 presents the values of (n) for all the glass samples, covering both methods. The change in density resulting from the increasing Dy_2O_3 content is responsible for the decrease in n, which enhances the transmission of light through the glass. The concentration of BO's directly impacts the density change, while the presence of Dy_2O_3 also plays a role in this phenomenon. The trend observed in [28] was also reported in this study .Lorentz-Lorenz relation was used to calculate the glass refractive index[29]:

$$\frac{n^2-1}{n^2+2} = 1 - \sqrt{\frac{E_g}{20}} \tag{3}$$

Based on E_{opt} one can calculate the electronegativity (χ) using [22]:

$$\chi = 0.2688\, E_g \tag{4}$$

Using the Eg values, the values of χ of the glass samples were obtained. The values of χ were increased with the increase of Dy_2O_3 contents from 0.75 to 1.25 mol% Table 2.

"Electro polarizability (α°)" & " optical basicity (Λ) " was calculated via [27]

$$\alpha^{\circ} = -0.9\,\chi + 3.5 \tag{5}$$

$$\Lambda = -0.5\,\chi + 1.7 \tag{6}$$

According to Table 2, as the Dy_2O_3 contents increased, the values for electronic polarizability and optical basicity of the glasses decreased, indicating inversely relationship for χ [22] ." According to Azlain et al.,[30] An increase in optical basicity indicates a decrease in electron donation capacity of oxide ions".

"The disorder of an amorphous material can be measured using Urbach's energy (Eu)[25]. Using the ASF method, the slope of the linear region in Figure 7 can be estimated by applying the following relation: [26]:

$$E_u = \frac{1239.83}{\text{slope}} \tag{7}$$

The addition of Dy_2O_3 caused a decrease in Eu values and an increase in E_{opt} as in Table 2. The main reason for this is the increased formation of BOs in the glass structure and the breakdown of NBOs.[31]. To summarize, as the Dy_2O_3 concentration increased, the NBO number decreased due to the increased presence of oxygen anions that promoted the formation of TeO_4 units. A lower Urbach energy in glass network structures is generally indicative of a decrease in disorders [32].Forming BOs and BO_4 units will become more, making the network structures more compact in the current glass system [33, 34].

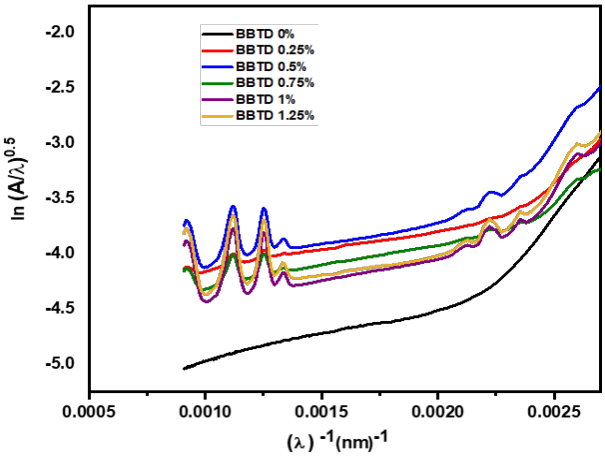

Fig. 7. $ln(A/\lambda)^{0.5}$ against $(1/\lambda)$ plot for the proposed glasses.

The steepness parameter (*S*) defines the interactions of electron-phonon or exciton-phonon [35] The growth of the UV absorption edge in the current glasses can be affected by the correlation of S and Eu, which was estimated using [25]:

$$S = \frac{T_B\, c}{E_u} \tag{8}$$

where c is the temperature and T_B is the constant of Boltzmann. Increasing the Dy_2O_3 content led to higher S values in the glasses. An inverse relation between S and E_u values was established Table 2.

Table 1. Values of λ_{cut}, Eg, and n of the glasses obtained using Tuac and ASF methods.

Sample code	Tauc's method			ASF method		
	λ_{cut} (nm)	$E_{Band}^{Tuac\,s,indirct}$ (eV)	n	λ^{-1} (nm^{-1})	$E_{Band}^{ASF,indirct}$ (eV)	n
BBTD 0%	431	2.8487	2.43905	0.0023	2.852	2.43811
BBTD 0.25%	452	2.6493	2.49854	0.00217	2.6958	2.48421
BBTD 0.5%	471	2.6337	2.50341	0.00213	2.647	2.49926
BBTD 0.75%	454	2.7435	2.46981	0.00212	2.752	2.46727
BBTD 1%	436	2.8225	2.44659	0.00228	2.827	2.44529
BBTD 1.25%	430	2.8867	2.42827	0.00232	2.876	2.43129

Table 2. The values of E_u, S, χ, $\propto_\circ$ and Λ of the glasses.

Sample code	E_u	S	χ	$\propto_\circ$	Λ
BBTD 0%	0.3062	0.084	0.7657	2.8108	1.3171
BBTD 0.25 %	0.3152	0.081	0.7121	2.8590	1.3439
BBTD 0.5%	0.3228	0.079	0.7079	2.8628	1.3460
BBTD 0.75%	0.3138	0.0820	0.7374	2.8362	1.3312
BBTD 1%	0.3045	0.0845	0.7586	2.8171	1.3206
BBTD 1.25%	0.3001	0.0857	0.7759	2.8016	1.3120

3.3. Gamma rays shielding characteristics of glasses

Figures 8 to 15 display the comparison between the theoretical and experimental values of various radiation shielding parameters of the studied glasses. The experimental setup for this study involved the use of a thallium-doped sodium iodide detecto. The NaI(TI) detector is commonly employed for gamma-ray detection. Attenuation coefficient refers to the process of reducing the number of photons in a gamma-ray beam as it interacts with matter. This attenuation can occur through absorption, scattering, and pair production of the primary photons. The attenuation processes at low energies, specifically below 26 keV, are predominantly dominated by the photoelectric effect. However, in cases where higher energy photons interact with low Z materials, the dominant mechanism of attenuation is Compton scattering. In addition, it is important to note that at photon energies greater than 1.02 MeV, Pair production plays a significant role in the attenuation process. The attenuation coefficient can be classified into two types. The term that refers to the fraction of gamma rays that are absorbed per unit thickness of the material is called (LAC). It quantifies the attenuation or reduction in the level of gamma ray activity as they pass through a material. (LAC) is specific to each material and is dependent on factors such as the energy of the gamma rays and the atomic structure of the material. It is commonly expressed in units of cm^{-1} as Beer-Lambert law [36, 37]:

$$I = I_\circ \, e^{-\mu T} \tag{9}$$

where I_o and I are the corresponding incoming and outgoing gamma rays' intensity, and T is the thickness of glass (attenuator). In this work, ^{137}Cs and ^{60}Co sources were used for gamma rays at energies of "0.662, 1.173, and 1.333" MeV. The values of MAC were calculated using [38]:

$$\frac{\text{LAC}}{\rho} = \sum_i w_i \left(\frac{\text{LAC}}{\rho}_i\right) \tag{10}$$

From Fig. 8 and 9, it is observed that the increase in Dy_2O_3 content has a direct correlation with the increase in MAC. This can be attributed to two main factors. One of the primary reasons for the increase in MAC is the higher mass density observed in the samples after adding of Dy_2O_3 .The higher the mass density, the more probable it becomes for photons to interact with the material, ultimately leading to a greater attenuation of the radiation. Another point to consider is that Dysprosium, with an atomic number of 66, has a higher atomic number than the base material. The probability of photon interaction and subsequent radiation attenuation is higher in elements with higher atomic numbers. Higher amount of Dy_2O_3 in the samples leads to a boost in MAC. [39].

The HVL is a measure of the shielding effectiveness of a material against gamma radiation. It represents the thickness of a specific material that is required to attenuate the gamma rays by 50%. [40]. This relationship is expressed as follows[41, 42].

$$HVL = \frac{\ln 2}{LAC} \tag{11}$$

TLV values were estimated using[41, 42].

$$TVL = \frac{\ln 10}{LAC} \tag{12}$$

The HVL values for the studied glasses, both experimental and theoretical, are depicted in Figures 10 and 11. These figures demonstrate energy range variations of 0.66, 1.173, and 1.33 eV. Increasing the amount of Dy_2O_3 in the current glass system results in a noticeable decrease in HVL, demonstrating its enhanced efficiency in attenuating gamma radiation. Both the (LAC) and the type of material are important factors in determining the HVL of a material. Different materials have varying atomic structures and composition, leading to different interactions with photons. As an illustration, materials possessing high atomic numbers generally exhibit higher (LAC) because they provide increased possibilities for photon interactions.[43]. Furthermore, it is directly proportional to the energy of the photon and inversely proportional to the density of the material. [43]. TVL (Figure 12 and 13) values were increased with the increase of photon energy, this was due to the decrease of the LAC values of the prepared glasses with the increase of incident photon energy [44]. The effectiveness of the proposed glasses in shielding against X-rays and γ-rays can be determined by their higher LAC values and lower HVL and TVL values. [4]. Another important factor to mention is the (MFP) of a photon, which refers to the distance it can travel in a substance before another reaction happens[14]can be found through the following relationship[45].

$$MFP = \frac{1}{LAC} \tag{13}$$

Figure 14 and 15 illustrates the experimental and theoretical MFP values of the glasses against photon energy respectively. In the lower energy zone, LAC values were higher, showing an inverse relationship with MFP values. The density of the sample greatly affects the attenuation of gamma rays. Consequently, in my previous study [46], The examination revealed that a sample, which had a concentration of 1.25% mol of BBTD, exhibited a density of 4.772 g/cm3. In addition, this sample showcased the lowest HVL, TVL, and MFP measurements, while exhibiting the highest LAC & MAC measurements.

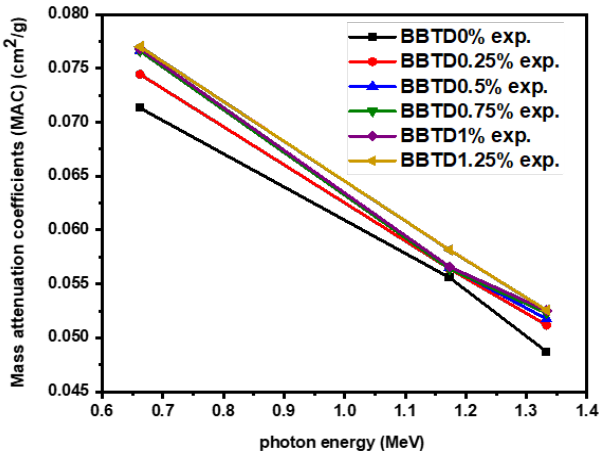

Fig. 8. Experimentally measured MAC of the prepared glasses.

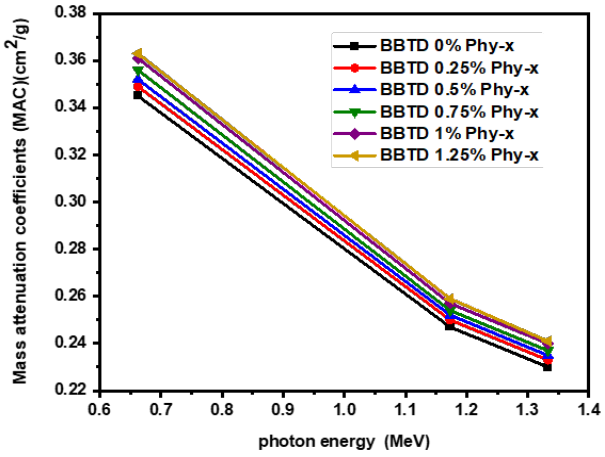

Fig. 9. Theoretically calculated MAC of the prepared glasses.

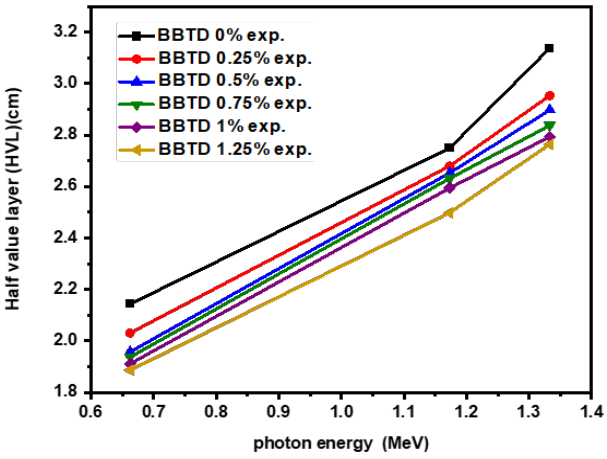

Fig. 10. Experimentally measured HVL values of prepared glasses.

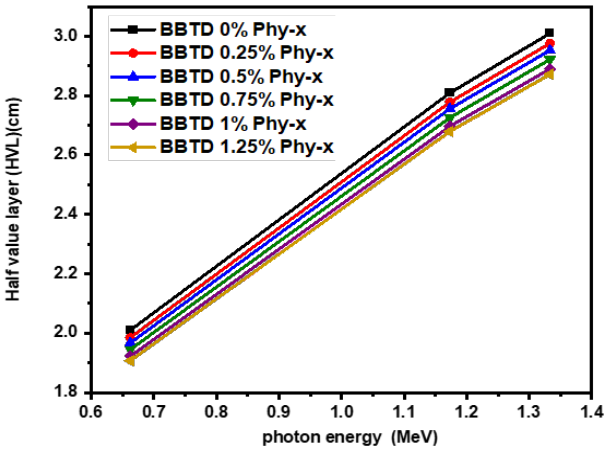

Fig. 11. Theoretically estimated HVL values of glasses.

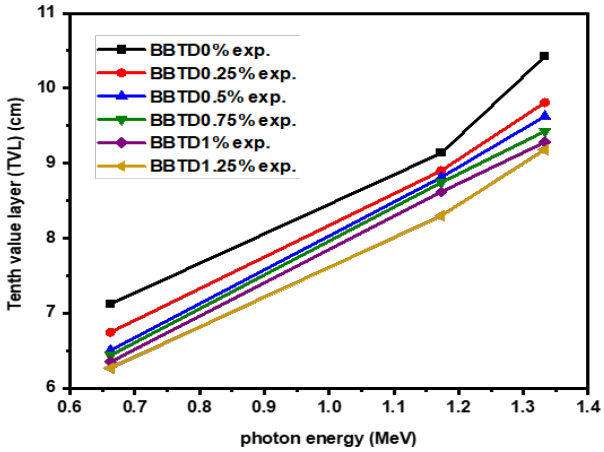

Fig. 12. Experimentally measured TVL of glasses.

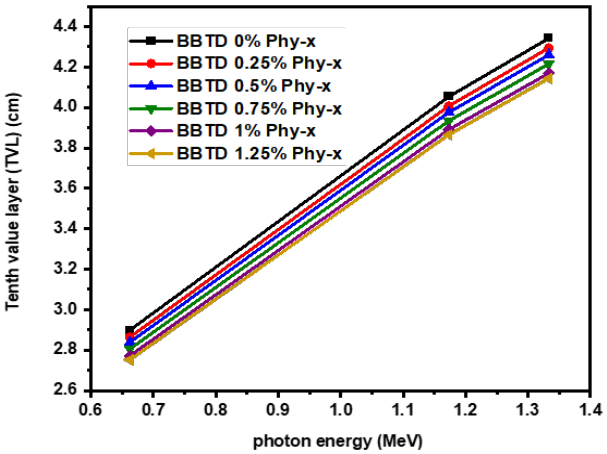

Fig. 13. Theoretically estimated TVL of glasses.

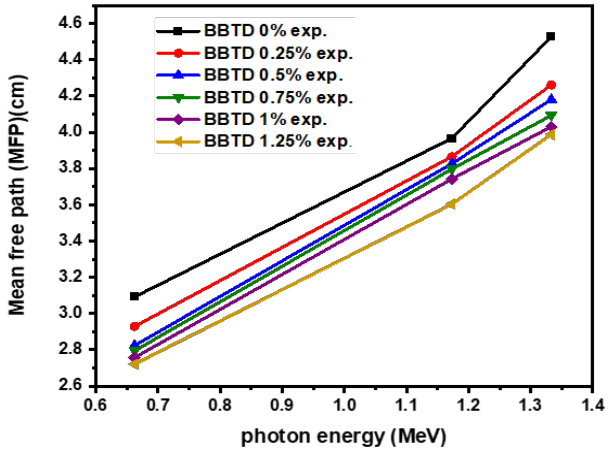

Fig. 14. Experimental MFP of glasses.

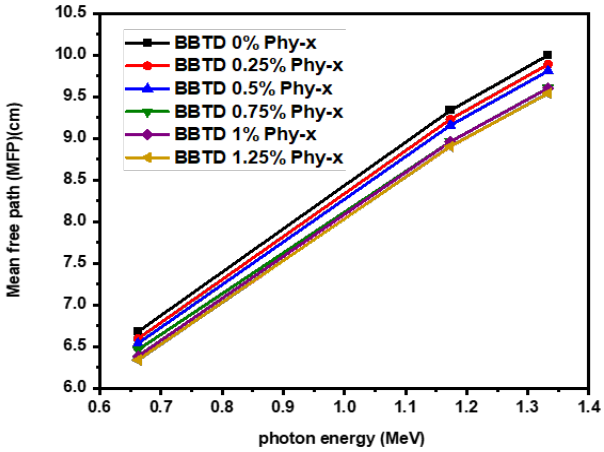

Fig. 15. Theoretical MFP of glasses.

4. Conclusion

An experimental and theoretical assessment was conducted for the first time to evaluate the effectiveness of Dy_2O_3-doped barium-boro-tellurite glasses in shielding gamma rays. Tauc's and ASF methods were utilized to estimate the E_{gap}^{Indir} and refractive index of the glasses, and the results showed a good agreement between the two methods. It was observed that the addition of Dy_2O_3 in the glasses led to an increase in their refractive index, this related to the converted TeO_3 into TeO_4 units, which occurred through the creation of BOs and readjustments in the glass network structures. Additionally, the inclusion of Dy_2O_3 led to a reduction in the electronic polarizability and optical basicity measurements of the glass.

These findings suggest that the glasses doped with Dy_2O_3 are suitable for the manufacturing of optical devices. Furthermore, the sources of gamma rays from ^{137}Cs and ^{60}Co (at energies of 0.662, 1.173, and 1.333 MeV) were used to test the radiation shielding capacity of the glasses. This was done by measuring parameters such as MAC, LAC, HVL, TVL, & MFP, which were then compared to theoretical estimates (Phy-x/PSD). It was found that the MAC values improved as the content of Dy_2O_3 increased. The HVL and LAC values showed an inverse proportional relationship, which was influenced by factors such as density, material type, and photon energy. Understanding these factors is crucial in various applications, including radiation protection and diagnostic imaging. The TVL values increased as the incident photon energy rose. The MFP values for all the synthesized glasses were very small when exposed to gamma ray photons, indicating their excellent ability to attenuate photons. Overall, the proposed glass composition is deemed advantageous for constructing radiation shields.

References

[1] Y. S. Rammah, A. A. Ali, R. El-Mallawany, and F. I. El-Agawany, "Fabrication, physical, optical characteristics and gamma-ray competence of novel bismo-borate glasses doped with Yb2O3 rare earth," Physica B: Condensed Matter, vol. 583, p. 412055, 2020/04/15/ 2020, doi: https://doi.org/10.1016/j.physb.2020.412055

[2] H. Tekin et al., "An investigation on shielding properties of different granite samples using MCNPX code," 2018.

[3] A. M. Abu El-Soad, M. I. Sayyed, K. A. Mahmoud, E. Şakar, and E. G. Kovaleva, "Simulation studies for gamma ray shielding properties of Halloysite nanotubes using MCNP-5 code," Applied Radiation and Isotopes, vol. 154, p. 108882, 2019/12/01/ 2019, doi: https://doi.org/10.1016/j.apradiso.2019.108882.
https://doi.org/10.1016/j.apradiso.2019.108882

[4] S. Kaur and K. J. Singh, "Investigation of lead borate glasses doped with aluminium oxide as gamma ray shielding materials," Annals of Nuclear Energy, vol. 63, pp. 350-354, 2014/01/01/ 2014, doi: https://doi.org/10.1016/j.anucene.2013.08.012.
https://doi.org/10.1016/j.anucene.2013.08.012

[5] Y. Rammah, K. Mahmoud, F. Q. Mohammed, M. Sayyed, O. Tashlykov, and R. El-Mallawany, "Gamma ray exposure buildup factor and shielding features for some binary alloys using MCNP-5 simulation code," Nuclear Engineering and Technology, vol. 53, no. 8, pp. 2661-2668, 2021.
https://doi.org/10.1016/j.net.2021.02.021

[6] M. Sayyed, G. Lakshminarayana, and M. Mahdi, "Evaluation of radiation shielding parameters for optical materials," Chalcogenide Lett, vol. 14, no. 2, pp. 43-47, 2017.

[7] M. Al-Buriahi et al., "Structure, optical, gamma-ray and neutron shielding properties of NiO doped B2O3-BaCO3-Li2O3 glass systems," Ceramics International, vol. 46, no. 2, pp. 1711-1721, 2020.
https://doi.org/10.1016/j.ceramint.2019.09.144

[8] R. El-Mallawany, "The optical properties of tellurite glasses," Journal of applied physics, vol. 72, no. 5, pp. 1774-1777, 1992.
https://doi.org/10.1063/1.351649

[9] I. Shaltout, Y. Tang, R. Braunstein, and E. Shaisha, "FTIR spectra and some optical properties of tungstate-tellurite glasses," Journal of Physics and Chemistry of Solids, vol. 57, no. 9, pp. 1223-1230, 1996.
https://doi.org/10.1016/0022-3697(95)00309-6

[10] D. Sushama and P. Predeep, "Thermal and optical studies of rare earth doped tungston-tellurite glasses," International Journal of Applied Physics and Mathematics, vol. 4, no. 2, p. 139, 2014.
https://doi.org/10.7763/IJAPM.2014.V4.271

[11] J.-C. Champarnaud-Mesjard, P. Thomas, P. Marchet, B. Frit, A. Chagraoui, and A. Tairi, "Glass formation study in the Bi2O3-TeO2-WO3 system," in Annales de Chimie Science des Matériaux, 1998, vol. 23, no. 1-2: Elsevier, pp. 289-292.
https://doi.org/10.1016/S0151-9107(98)80076-7

[12] D. Lezal, J. Pedlikova, P. Kostka, J. Bludska, M. Poulain, and J. Zavadil, "Heavy metal oxide glasses: preparation and physical properties," Journal of Non-Crystalline Solids, vol. 284, no. 1-3, pp. 288-295, 2001.
https://doi.org/10.1016/S0022-3093(01)00425-2

[13] N. S. Hussain et al., "Absorption and emission analysis of RE3+ (Sm3+ and Dy3+): lithium boro tellurite glasses," Journal of nanoscience and nanotechnology, vol. 9, no. 6, pp. 3672-3677, 2009.
https://doi.org/10.1166/jnn.2009.NS49

[14] Y. Rammah, A. Ali, R. El-Mallawany, and F. El-Agawany, "Fabrication, physical, optical characteristics and gamma-ray competence of novel bismo-borate glasses doped with Yb2O3 rare earth," Physica B: Condensed Matter, vol. 583, p. 412055, 2020.
https://doi.org/10.1016/j.physb.2020.412055

[15] F. Mohd Fudzi, H. Mohamed Kamari, A. Abd Latif, and A. Muhammad Noorazlan, "Linear optical properties of zinc borotellurite glass doped with lanthanum oxide nanoparticles for optoelectronic and photonic application," Journal of Nanomaterials, vol. 2017, 2017.
https://doi.org/10.1155/2017/4150802

[16] S. Zaidan, M. Al-Hilli, and D. Mahdi, "The effects of additives in to heat treatment temperature and time on the crystallinity of lithium silicate glass-ceramic," in IOP Conference Series: Materials Science and Engineering, 2020, vol. 757, no. 1: IOP Publishing, p. 012060.
https://doi.org/10.1088/1757-899X/757/1/012060

[17] L. Escobar-Alarcón, A. Arrieta, E. Camps, S. Muhl, S. Rodil, and E. Vigueras-Santiago, "An alternative procedure for the determination of the optical band gap and thickness of amorphous carbon nitride thin films," Applied surface science, vol. 254, no. 1, pp. 412-415, 2007.

https://doi.org/10.1016/j.apsusc.2007.07.052

[18] J. Tauc, "Amorphous and liquid semiconductors plenum," Springer, London, vol. 10, pp. 978-1, 1974.
https://doi.org/10.1007/978-1-4615-8705-7

[19] A. Lösche, "NF MOTT, EA DAVIS. Electronic Processes in Non-Crystalline Materials Clarendon-Press, Oxford 1971 437 Seiten.£ 7, 50," ed: Wiley Online Library, 1972.
https://doi.org/10.1002/crat.19720070420

[20] D. Souri and K. Shomalian, "Band gap determination by absorption spectrum fitting method (ASF) and structural properties of different compositions of (60− x) V2O5-40TeO2-xSb2O3 glasses," Journal of Non-Crystalline Solids, vol. 355, no. 31-33, pp. 1597-1601, 2009.
https://doi.org/10.1016/j.jnoncrysol.2009.06.003

[21] Y. Al-Hadeethi, M. Sayyed, and Y. Rammah, "Fabrication, optical, structural and gamma radiation shielding characterizations of GeO2-PbO-Al2O3-CaO glasses," Ceramics International, vol. 46, no. 2, pp. 2055-2062, 2020.
https://doi.org/10.1016/j.ceramint.2019.09.185

[22] R. El-Mallawany, W. Abou-Taleb, M. Naeem, M. Krar, and S. Talaat, "Synthesis, physical, optical properties and gamma-ray shielding parameters of some tellurite glasses," Optik, vol. 242, p. 167171, 2021.
https://doi.org/10.1016/j.ijleo.2021.167171

[23] S. Khor, Z. Talib, and W. M. Yunus, "Optical properties of ternary zinc magnesium phosphate glasses," Ceramics International, vol. 38, no. 2, pp. 935-940, 2012.
https://doi.org/10.1016/j.ceramint.2011.08.013

[24] A. Abouhaswa, H. M. Zakaly, S. A. Issa, M. Pyshkina, R. El-Mallawany, and M. Y. Mostafa, "Lead borate glasses and synergistic impact of lanthanum oxide additive: optical and nuclear radiation shielding behaviors," Journal of Materials Science: Materials in Electronics, vol. 31, pp. 14494-14501, 2020.
https://doi.org/10.1007/s10854-020-04009-y

[25] S. B. Kolavekar and N. Ayachit, "Impact of Pr2O3 on the physical and optical properties of multi-component borate glasses," Materials Chemistry and Physics, vol. 257, p. 123796, 2021.
https://doi.org/10.1016/j.matchemphys.2020.123796

[26] M. A. Algradee, E. E. Saleh, T. M. E. Sherbini, and R. El-Mallawany, "Optical and gamma-ray shielding features of Nd3+ doped lithium-zinc-borophosphate glasses," Optik, vol. 242, p. 167059, 2021.
https://doi.org/10.1016/j.ijleo.2021.167059

[27] M. Algradee, M. Sultan, O. Samir, and A. E. B. Alwany, "Electronic polarizability, optical basicity and interaction parameter for Nd 2 O 3 doped lithium-zinc-phosphate glasses," Applied Physics A, vol. 123, pp. 1-12, 2017.
https://doi.org/10.1007/s00339-017-1136-6

[28] N. Bhardwaj, A. Gaur, and K. Yadav, "Effect of doping on optical properties in BiMn1−x(TE)xO3 (where x = 0.0, 0.1 and TE = Cr, Fe, Co, Zn) nanoparticles synthesized by microwave and sol-gel methods," Applied Physics A, vol. 123, no. 6, p. 429, 2017/05/20 2017,
https://doi.org/10.1007/s00339-017-1042-y

[29] S. Hathot, B. Al Dabbagh, and H. Aboud, "Structural and spectroscopic correlation in barium-boro-tellurite glass hosts: effects of Dy 2 O 3 doping," Chalcogenide Letters, vol. 21, no. 2, 2024.
https://doi.org/10.15251/CL.2024.212.201

[30] M. Azlan, "Linear and non-linear optical properties of Zinc Borotellurite Glass Doped with Erbium, Erbium Nanoparticles, Neodymium and Neodymium Nanoparticles," PhD. dissertation, Universiti Putra Malaysia, Serdang, Malaysia, 2016.
https://doi.org/10.1016/j.jlumin.2016.09.047

[31] S. Hajer, M. Halimah, Z. Azmi, and M. Azlan, "OPTICAL PROPERTIES OF ZINC-BOROTELLURITE DOPED SAMARIUM," Chalcogenide Letters, vol. 11, no. 11, 2014.

[32] M. Halimah, W. Daud, H. Sidek, A. Zaidan, and A. Zainal, "Optical properties of ternary

tellurite glasses," Mater. Sci. Pol, vol. 28, no. 1, pp. 173-180, 2010.

[33] M. Halimah, M. Faznny, M. Azlan, and H. Sidek, "Optical basicity and electronic polarizability of zinc borotellurite glass doped La3+ ions," Results in physics, vol. 7, pp. 581-589, 2017. https://doi.org/10.1016/j.rinp.2017.01.014

[34] H. K. Obayes, R. Hussin, H. Wagiran, and M. A. Saeed, "Strontium ion concentration effects on structural and spectral properties of Li4Sr(BO3)3 glass," Journal of Non-Crystalline Solids, vol. 427, pp. 83-90, 2015/11/01/ 2015, https://doi.org/10.1016/j.jnoncrysol.2015.07.026

[35] R. Vettumperumal, S. Kalyanaraman, B. Santoshkumar, and R. Thangavel, "Estimation of electron-phonon coupling and Urbach energy in group-I elements doped ZnO nanoparticles and thin films by sol-gel method," Materials Research Bulletin, vol. 77, pp. 101-110, 2016/05/01/ 2016, doi: https://doi.org/10.1016/j.materresbull.2016.01.015

[36] A. M. A. Mostafa et al., "PbO-Sb2O3-B2O3-CuO glassy system: Evaluation of optical, gamma and neutron shielding properties," Materials Chemistry and Physics, vol. 258, p. 123937, 2021/01/15/ 2021, https://doi.org/10.1016/j.matchemphys.2020.123937

[37] H. O. Tekin, V. P. Singh, and T. Manici, "Effects of micro-sized and nano-sized WO3 on mass attenauation coefficients of concrete by using MCNPX code," Applied Radiation and Isotopes, vol. 121, pp. 122-125, 2017/03/01/ 2017, https://doi.org/10.1016/j.apradiso.2016.12.040

[38] F. Akman, M. Kaçal, M. Sayyed, and H. Karataş, "Study of gamma radiation attenuation properties of some selected ternary alloys," Journal of Alloys and Compounds, vol. 782, pp. 315-322, 2019. https://doi.org/10.1016/j.jallcom.2018.12.221

[39] A. Alalawi, M. S. Al-Buriahi, and Y. S. Rammah, "Radiation shielding properties of PNCKM bioactive glasses at nuclear medicine energies," Ceramics International, vol. 46, no. 10, Part A, pp. 15027-15033, 2020/07/01/ 2020, https://doi.org/10.1016/j.ceramint.2020.03.033

[40] I. Akkurt, B. Mavi, K. Gunoglu, H. Akyıldırım, and H. Canakci, "Photon Attenuation Coefficients of Iron Doped Clay at 662~ keV," Acta Physica Polonica A, vol. 123, no. 2, pp. 343-344, 2013. https://doi.org/10.12693/APhysPolA.123.343

[41] E. Kavaz et al., "The Mass stopping power/projected range and nuclear shielding behaviors of barium bismuth borate glasses and influence of cerium oxide," Ceramics International, vol. 45, no. 12, pp. 15348-15357, 2019. https://doi.org/10.1016/j.ceramint.2019.05.028

[42] I. Bulus, S. Dalhatu, M. Isah, R. Hussin, and E. Soje, "Structural and luminescence characterization of lithium-borosulfophosphate glasses containing dysprosium ions," Science World Journal, vol. 12, no. 4, pp. 98-101, 2017.

[43] M. A. Algradee, E. E. Saleh, T. M. El Sherbini, and R. El-Mallawany, "Optical and gamma-ray shielding features of Nd3+ doped lithium-zinc-borophosphate glasses," Optik, vol. 242, p. 167059, 2021/09/01/ 2021, https://doi.org/10.1016/j.ijleo.2021.167059

[44] I. C. Nnorom, O. Osibanjo, and M. O. C. Ogwuegbu, "Global disposal strategies for waste cathode ray tubes," Resources, Conservation and Recycling, vol. 55, no. 3, pp. 275-290, https://doi.org/10.1016/j.resconrec.2010.10.007

[45] M. J. Aldhuhaibat, H. S. Farhan, R. H. Hassani, H. M. Tuma, H. Bakhtiar, and A. Salim, "Gamma photons attenuation features of PbO-doped borosilicate glasses: a comparative evaluation," Applied Physics A, vol. 128, no. 12, p. 1058, 2022. https://doi.org/10.1007/s00339-022-06216-2

[46] S. F. Hathot, B. M. Al dabbagh, and H. Aboud, "Effects of Dy2O3 doping on physical and

mechanical characteristics of B2O3-TeO2-BaO glass," Engineering and Technology Journal, pp. 1-10, 2024, https://doi.org/10.30684/etj.2024.145037.1649